

# Magnetoquantum oscillations and confinement effects in arrays of 270-nm-diameter bismuth nanowires

T. E. Huber and K. Celestine

*Laser Laboratory, Howard University, Washington, DC 20059-0001, USA*

M. J. Graf

*Department of Physics, Boston College, Chestnut Hill, Massachusetts 02467, USA*

(Received 13 March 2003; published 20 June 2003)

We present a study of the electrical transport properties of 270-nm-diameter bismuth nanowire arrays embedded in an alumina matrix which are capped with layers of bulk Bi to produce a very low contact resistance. The resistance of the Bi nanowires has been measured over a wide range of temperatures (1.8–300 K) and magnetic fields (–8–8 T) for the longitudinal and transverse orientation. At low magnetic fields, the longitudinal magnetoresistance exhibits field-periodic modulations whose periods are consistent with theoretical predictions for the Aharonov-Bohm “whispering gallery” modes of electrons with long mean free path. At high magnetic fields, as the carrier cyclotron radius becomes smaller than the wire diameter, we observe Shubnikov–de Haas oscillations associated with both holes and electrons. These represent a detailed study of magnetoquantum oscillations in high-density nanowire arrays. Overall, the hole periods are increased by 5% and the carrier density is decreased by 13% from the values for bulk Bi, which is consistent with recent theoretical estimates of the effect of confinement on the carrier’s Fermi surface.

DOI: 10.1103/PhysRevB.67.245317

PACS number(s): 72.15.–v, 73.21.Hb, 73.23.Ad

## I. INTRODUCTION

Bi is a semimetal with unusual transport properties. These properties derive from its highly anisotropic Fermi surface, low carrier densities, small carrier effective masses, and long carrier mean free path. The elongated Fermi surfaces and small effective masses lead to a long Fermi wavelength ( $\lambda_F$ ) of about 600 Å, as opposed to a few Å in most metals.<sup>1</sup> The carrier mean free path in single-crystal Bi can be as long as a millimeter at 4.2 K, which is several orders of magnitude larger than the carrier mean free path for most metals.<sup>2</sup> Because of these long characteristic lengths, Bi has been extensively utilized for the study of quantum transport and finite-size effects. Early theoretical studies of metallic fine wires focused on classical size effects that appear when the electron mean free path  $l_e$  is limited at low temperatures by the carrier’s scattering at walls and grain boundaries.<sup>3</sup> It was observed that the resistance of fine metal wires decreases upon application of a magnetic field, and Chambers’ theory was introduced to account for this effect.<sup>4</sup>

Theoretical study has shown that when charge carriers pass through a cylindrical electrical conductor aligned with a magnetic field, their wavelike nature manifests itself through oscillatory behavior in the resistance as a function of the applied magnetic field. There are two types of quantum-size effects in normal conductors of long carrier’s mean free path that cause an oscillation of the magnetoresistance with a period ( $\Delta B$ ) that is proportional to  $\Phi_0/S$ , where  $S$  is the wire cross section and  $\Phi_0 = hc/e$  is the flux quantum, and which we collectively designated the Aharonov-Bohm (AB) effect. The first effect, Dingle oscillations, results from quantization of the electron energy spectrum. As the magnetic field is varied, the discrete energy levels cross the Fermi energy ( $E_F$ ) of the electron gas and thereby cause oscillations of the

resistance in a series of magnetic fields,  $B = \kappa\Phi_0/S$ , where  $\kappa$  assumes a set of values between about 0.9 and 2.2.<sup>5</sup> The second type of oscillation, with a period  $\Delta B = \Phi_0/S$ , is caused by electrons undergoing continuous grazing incidence at the wire walls. These are termed “whispering gallery” modes in an analogy to the acoustical phenomenon.<sup>6</sup> Brandt *et al.* discovered AB oscillations of this type in single nanowires grown by the Ulitovskii technique with diameters as small as 200 nm.<sup>7</sup> The oscillation period as a function of the angle between the magnetic field and the wire was investigated for wires with diameters between 560 and 800 nm and was found to be in agreement with the dependence expected for whispering gallery modes.<sup>8</sup> The study of these oscillations is important because they offer insight about the low-energy excitations of the electronic ground state of quantum wires.

A different type of oscillations, Shubnikov–de Haas (SdH) oscillations, results from the quantization of closed electronic orbits of diameter  $d_o < d$ , with  $d$  being the wire diameter, in a strong magnetic field, i.e., Landau levels; the oscillation period is  $\Delta(1/B) = e/(cA_e)$ , where  $A_e$  is any external cross-sectional area of the Fermi surface.<sup>9</sup> The SdH oscillations can reveal detailed information about the structure of the Fermi surface, and since confinement causes drastic modifications of the Fermi surface, the study of these oscillations can be of great potential in understanding the properties of the nanowires. Brandt *et al.*<sup>7</sup> observed SdH oscillations in their single nanowires and reported no deviations of the peak positions from the bulk Bi values, even for 200-nm wires. SdH oscillations also have been observed in high quality, 50-nm-thick Bi films, and the results have been interpreted in terms of an increase of the carrier density.<sup>10</sup>

The difficulty of fabricating fine Bi nanowires has been a major hindrance for these studies. Arrays of Bi nanowire

have been fabricated by a nonlithographic approach by using either vacuum impregnation or high-pressure injection of molten Bi into insulating nanochannel templates,<sup>11</sup> and long wires as small as 6 nm in diameter have been synthesized.<sup>12–14</sup> Clearly, the fabrication of Bi nanowire arrays is a stepping stone toward the fabrication of single Bi nanowires of the same diameter. In contrast, the Ulitovskii technique has not progressed below the 100–200-nm barrier in 25 years. However, the characterization of Bi wire arrays is still preliminary, and it is not clear if one can produce arrays of sufficient uniformity and quality to allow a detailed study of the magneto-oscillatory behavior. Measurements of the transverse magnetoresistance [TMR= $R(T,B)/R(T,0)$ ] of 200-nm-diameter wire arrays have been presented, and the results have been interpreted in terms of size effects.<sup>14–16</sup> The longitudinal magnetoresistance (LMR) and TMR of wire arrays with wire diameters between 60 and 110 nm have also been measured, and the results have been interpreted in terms of a classical size effect and weak localization theories.<sup>14</sup> The LMR of Bi wire arrays with diameters ranging from 7 to 200 nm prepared using vacuum impregnation has been interpreted in terms of the interplay between the electron cyclotron radii, electron scattering at the wire's walls, size-induced energy level quantization, and the transfer of carriers between the different carrier pockets of the Fermi surface.<sup>16</sup> The effect of impurities on the transport properties of Bi nanowires has been studied also, particularly the case of Te,<sup>13</sup> an electron acceptor. The effect of Cu impurities introduced through the contact material has also been investigated.<sup>14</sup> Electrochemical growth has also been employed to grow nanowire arrays in templates of various types.<sup>17</sup> So far, these studies of nanowire arrays have yielded evidence for size effects, but there have been no detailed studies regarding SdH oscillations<sup>18</sup> and AB effects have not been previously observed. As we will show, magnetoquantum oscillations are also observable in high quality Bi nanowire arrays.

The small effective masses and large spatial extent of the electron wave function makes confinement of the electron gas in the directions transverse to the wire's length apparent in wires with diameters in the tens and hundreds of nanometers. There is interest in the semimetal-semiconductor transition of very thin Bi films<sup>19</sup> and wires,<sup>13</sup> which is proposed to result from quantum confinement. Since the electron motion in the quantum wires is restricted in directions normal to the wire axis, the quantum confinement causes the energies associated with the transverse motion to be quantized, and the electron and hole energy levels are shifted. The effective band overlap energy ( $E_0$ ) between the lowest  $L$ -point electron subband and the highest  $T$ -point hole subband is 37 meV for bulk Bi. In nanowires of diameter  $d$ ,  $E_0$  is decreased<sup>13</sup> and the shift  $\Delta E_0$  is given by

$$\Delta E_0 = -\frac{2\hbar^2\chi_{10}^2}{m_{\text{ch}}d^2} - \sqrt{\frac{E_{gL}^2}{4} + E_{gL}\frac{2\hbar^2\chi_{10}^2}{m_{\text{ce}}d^2}} + \frac{E_{gL}}{2}. \quad (1)$$

The first term in Eq. (1) reflects the parabolic approximation used to describe the highest  $T$ -point hole subband, where  $m_{\text{ch}}$  is the cyclotron effective mass of holes.  $\chi_{10}$  is the first

root of the Bessel function of order 1 ( $\chi_{10}=3.83$ ). The second term is due to the increase of the lowest  $L$ -point electron subband.  $E_G$  is the electron energy gap ( $E_{gL}=15$  meV), and  $m_{\text{ce}}$  is the cyclotron effective mass of electrons. Values for  $m_{\text{ch}}$  and  $m_{\text{ce}}$  are dependent upon the crystalline orientation of the Bi in the nanowires. For very small diameters,  $E_0$  changes sign and the semimetal-to-semiconductor transition is predicted to occur. The critical wire diameter for Bi nanowires oriented along the trigonal direction is around 33 nm within the cyclotron mass approximation. Quantum confinement provides a practical way to manipulate the electronic properties by changing the electronic density of states. This leads to a wide range of opportunities for utilizing the electronic properties of the resulting one-dimensional system for various practical device applications. Bi nanowires are of special interest for thermoelectric applications, as Bi and its alloys have the largest figure of merit of any material at 100 K.<sup>20</sup> Theoretical studies show a one-dimensional material to potentially exhibit a significant increase of the thermoelectric figures of merit.<sup>21</sup>

In this work, we present our results for the magnetotransport on Bi nanowire arrays with average wire diameters of 270 nm, a size comparable to that of wires used in Brandt's early work. Our polycrystalline nanowires have a high degree of orientation along the trigonal axis, and these nanowires are terminated in bulk Bi to minimize contact resistance effects. We clearly observed magnetoquantum oscillations, a fact which points to the high quality and high degree of uniformity of our nanowires. At high fields, when the cyclotron radius ( $r_c$ ) is smaller than the wire diameter ( $d$ ), Shubnikov-de Haas oscillations are evident, and modifications of the SdH periods from their bulk values result from spatial confinement effects. These modifications are consistent with the proposed semimetal-semiconductor transition expected in Bi for sufficiently small wire diameters. At lower fields, when  $r_c > d/2$ , we see indications of AB whispering-gallery modes.

In Sec. II, we describe the sample fabrication and characterization. In Sec. III, the experimental procedures for the transport measurements are described and the magnetoresistance data are presented. We discuss the magnetoresistance results in Sec. IV and summarize the paper in Sec. V. In the Appendix, we discuss the four-contact probe method as it applies to Bi-capped nanowire arrays.

## II. SAMPLE PREPARATION AND CHARACTERIZATION

The Bi nanowire arrays are fabricated by the template injection technique as described in detail elsewhere.<sup>22</sup> In most cases, molten metals do not wet glass or alumina, and an external pressure is required to force impregnation of the insulating perform with a liquid metal. The Washburn equation ( $P = -2\gamma_{\text{lv}} \cos \theta/R$ ) describes this pressure, where  $R$  is the pore radius,  $\theta$  is the contact angle between the liquid metal and the insulator surface, and  $\cos \theta = (\gamma_{\text{sv}} - \gamma_{\text{sl}})/\gamma_{\text{lv}}$ , with  $\gamma_{\text{sv}}$ ,  $\gamma_{\text{sl}}$ , and  $\gamma_{\text{lv}}$  representing the solid-vapor, solid-liquid, and liquid-vapor surface energies, respectively. The wetting behavior, which is characterized by the contact angle between the liquid metal and the solid surface, determines

the value of the impregnation pressure. For  $\theta > 90^\circ$ , the system is nonwetting. Since values for the surface tension ( $\gamma_{lv}$ ) of liquid metals and semiconductors span the range from 100 to 600 dyne/cm, the processing pressure is typically in the range of a kilobar. Conversely, a minimum pore size exists for impregnation assisted by a finite applied pressure ( $P$ ). For Bi, it is found that an externally applied hydrostatic pressure is needed to overcome the surface tension effects, indicating that, for molten Bi on alumina,  $\theta > 90^\circ$ . The surface tension of liquid Bi,  $\gamma_{lv}$ , has been measured by the bubble pressure method, and has been found to be 380 dyne/cm at its melting point (270 °C). The surface tension decreases slightly for increasing temperatures with a linear temperature coefficient of  $-0.14$  dyne  $\text{cm}^{-1} \text{C}^{-1}$ . Assuming the least favorable case of complete nonwetting ( $\theta = 180^\circ$ ), Washburn's equation gives  $d = 15.2/P$ , where  $P$  is measured in kilobars and  $d$  is the pore diameter in nanometers. Thus, for a modest applied pressure of 0.1 kbar, all channels larger than 152 nm in diameter will be filled with liquid Bi.

The alumina templates used in this work are sold commercially for microfiltration under the trade name Anapore<sup>23</sup> and are made by the anodization of aluminum; they are sold with a nominal 200-nm channel diameter. The template consists of an alumina plate that is 25 mm in diameter and about 55  $\mu\text{m}$  thick, which supports an array of parallel, largely noninterconnected, cylindrical channels running perpendicular to the plate surface. We performed a careful study of the morphology of the channels in the template. The channel structure is slightly asymmetric, with the channels tapering toward the plate surface that was originally in contact with the aluminum metal. The channel ends are also irregular on this side, over a length of about 2  $\mu\text{m}$  from the surface; this defect was removed by mechanical polishing. The average channel diameter near each surface of the anodic alumina plate, after removal of the surface layer, is  $235 \pm 30$  nm and  $310 \pm 40$  nm. Note that the channels have the shape of a funnel and that the error bars indicate that the funnels are very similar to each other in size and shape.<sup>24</sup>

For our injection process, the nanochannel alumina was cleaned by boiling in solutions of 30%  $\text{H}_2\text{O}_2$ , rinsing in boiling deionized water, and drying at 150 °C in a vacuum. The alumina plates and the Bi (purity, 99.999%) were packed in a thin-wall metal tube with a quartz liner sealed at the bottom. The metal ampoule was then inserted into the reactor of a high-temperature/high-pressure injection apparatus and was vacuum dried at 200 °C for a half hour. The Bi injection was done at 340 °C and 2 kbar. When the injection was complete, the reactor was cooled slowly over a period of 1 h and the impregnant solidified inside the channels; the pressure was then released. We believe that this slow cooldown acts to anneal the Bi. The sample was extracted from the ampoule, and standard abrasion techniques were used to remove the surrounding excess impregnant. The composite is easily distinguished from the surrounding Bi because it is not as shiny. This processing was performed in such a way that the layers of bulk Bi that are adjacent to the template surfaces were left undisturbed. The Bi caps are typically a few hundred microns thick. Samples for this study were exposed to ambient air for several months; we found that sample degra-

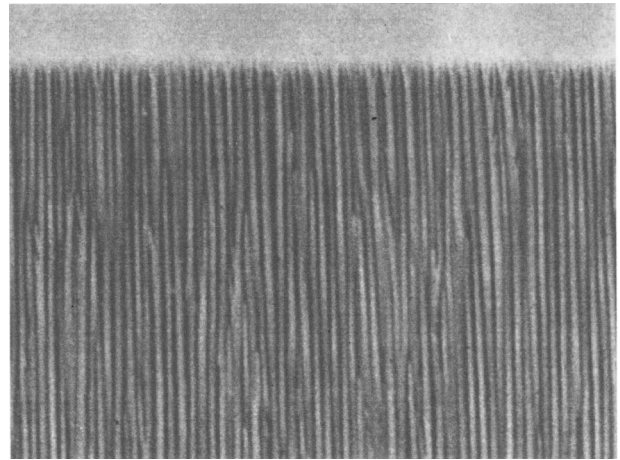


FIG. 1. SEM cross section of a 200-nm (nominal) wire array. The wires appear as the light areas; the dark areas are the insulating matrix.

dation was not a concern, and the repeatability of the measurements between different runs for the same sample was excellent.

The structure of the nanowire arrays was examined by scanning electron microscopy (SEM) and x-ray diffraction (XRD). An SEM image of the Bi wire arrays is shown in Fig. 1; it was obtained with a Cameca Electron Microprobe, model MBX, and taken using secondary electron imaging. Microprobe elemental composition analysis indicates that the Bi is free of common impurities. Our SEM examination of the interface between the nanowire array and the Bi caps shows that this interface layer is continuous. Therefore we assumed that we were making electrical contact to all the nanowires through these caps. We also examined the crystal-line structure of the arrays of nanowires with the Bi caps removed by etching. The XRD spectra peaks were very narrow, which indicated a long-range periodicity of the structure along the wire length.<sup>25</sup> The positions of the observed peaks corresponded within the experimental resolution ( $0.2^\circ$ ) with those for the bulk, indicating that the rhombohedral crystal structure of bulk Bi is preserved in the nanowires. The appearance of only a few peaks of the rhombohedral structure suggested that individual wires are composed of highly oriented crystalline grains. The prominence of the (003), (006), and (009) peaks relative to the (102) peak indicated that the crystal grains are oriented with the trigonal axis along the wire length, since the scattering geometry employed probes only interplanar distances along the wire length. There were no shifts in the peak positions, and we estimate that any changes in the lattice parameters ( $\Delta a/a$ ) would be  $< 1.7 \times 10^{-3}$ . By comparison, the majority of the Bi nanowire arrays in all cases in Refs. 13 and 16 were oriented along a crystal direction perpendicular to the (202) lattice plane, i.e., the wire axis lies along a trigonal-bisectrix plane and close to the bisectrix. The different growth techniques used may account for the different crystalline orientations among samples from various sources.

### III. EXPERIMENTAL RESULTS

Measurements of the zero-field resistance and of the magnetoresistance of the polycrystalline bulk Bi material sur-

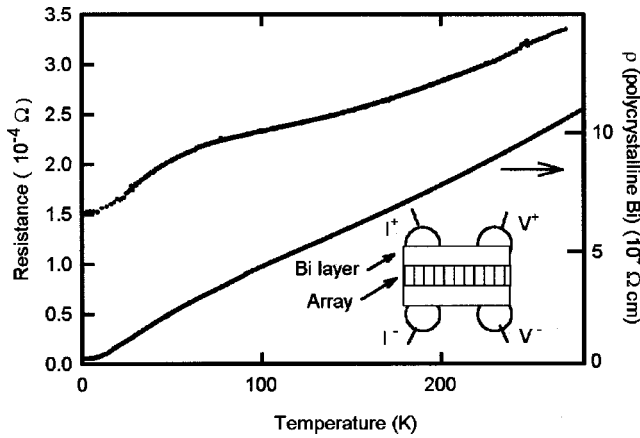


FIG. 2. Temperature dependence of the resistance of the 200-nm (nominal) wire array and of the resistivity of the Bi contact layer material. The inset shows a schematic of the arrangement of electrodes used for the transport measurements.

rounding the nanowire samples and of the nanowires themselves were made in a  $^4\text{He}$  gas-flow cryostat operating in a temperature range of 1.8–300 K and for a magnetic field range of  $-8$ – $8$  T. We employed both direct current (dc) and 17-Hz alternating current (ac) techniques where current is injected between two silver epoxy electrodes lying on opposite sides of the wire array, and the voltage was measured between the other pair of electrodes which are also on opposite sides of the wire array. Both dc and ac techniques yielded equivalent results. The inset of Fig. 2 shows a schematic of the electrode arrangement. The measuring current is typically 10 mA. Variation of the excitation amplitude showed that there was no self-heating of the samples.

Transport measurements on the actual Bi nanowire arrays are essentially two-point measurements, and the measured resistance contains a contribution from the resistance at the boundary between the contact material and the Bi nanowires which is due to the contact resistance of the individual nanowires and the contact area and also effectively depends upon the number of wires that are contacted. The contact resistance between nanowires and a bulk material and its dependence with magnetic field has been studied in the past,<sup>18</sup> including the case of nanowires of copper and aluminum on bulk Bi at low temperatures. The resistance of a point contact of diameter  $d$  can be thought of as a series resistance of a ballistic component, the Sharvin resistance ( $R_{\text{sh}} = 4\rho l_e / 3\pi d^2$ ), where  $\rho$  is the resistivity of bulk Bi,  $l_e$  is the mean free path, and a diffusive component, the Maxwell resistance ( $R_M$ ), which is  $\rho/2d$ . These two expressions are the limiting cases for a pure contact ( $l_e > d$ ),<sup>26</sup> and a dirty contact ( $l_e < d$ ), respectively. The Maxwell contribution is negligible at low temperatures and in the absence of a magnetic field because the resistivity of pure Bi is very small. However, the Sharvin term is significant—for a single nanowire, we determined that the value of  $R_{\text{sh}}$  was  $10 \Omega$  for a diameter of 200 nm and that  $\rho l_e$  had a value of  $10^{-8} \Omega \text{ cm}^2$ . Both contributions to the contact resistance increase with applied magnetic field, particularly the Maxwell term since it is proportional to the bulk resistivity (not the product  $\rho l_e$ ),

which has a large magnetic-field dependence. At first sight, it would appear that  $R_{\text{sh}}$  exhibits no oscillations with the magnetic field because the product  $\rho l_e$  is largely independent of magnetic field in the ordinary Drude approximation. However, the expression for  $R_{\text{sh}}$  as given above has to be modified to account for the modification of the electronic density of states with magnetic field and for diffraction effects.<sup>18,27</sup> Contact resistance issues are also relevant in other small-size systems such as carbon nanotubes.<sup>28</sup> In view of these various effects arising at the contacts, it is apparent that every precaution should be taken to minimize contact resistance. The contact resistance is undoubtedly reduced if the Bi nanowires are terminated in a bulk Bi layer (i.e., the cap), since the scattering at the contact is minimized on account of the continuation of the lattice structure at the interface between the nanowire and contact. This is the approach taken here with the following added benefits: (i) the contact between a Bi nanowire and bulk Bi can be considered a standard of contact resistance to Bi nanowires, in comparison to the contact resistance between pairs of dissimilar materials (e.g., Bi nanowires and bulk silver), and (ii) the contact area is very close to the diameter of the nanowire. Clearly, progress in the science and in the application of nanowires to, for example, thermoelectricity, is closely associated with the issue of contact resistance. Our nanowires are capped with a layer of Bi as shown in the inset of Fig. 2; in this way, the number of wires contacted is maximized and the contact resistance to the individual nanowires is minimized. We find that the residual (low-temperature) contact resistance of our samples is less than  $10^{-4} \Omega$ . This is consistent with the single-nanowire results, considering that the array consists of  $5 \times 10^8$  wires in parallel. In comparison, the resistance of samples with contacts prepared through other approaches ranges from  $10^2$  to  $10^4 \Omega$ , which indicates that the contact to the electrodes is not continuous<sup>13,16</sup> and that a small number of nanowires is contacted.

In order to leave the Bi layer cap intact, we abraded the sample in the form of a parallelepiped using alumina powder; the four sides parallel to the wires in the array were polished to expose the nanowire template. The two sides perpendicular to the wires in the array, of length  $L$  and width  $W$  (both dimensions, 1 mm), are abraded enough to leave the smooth layer of bulk Bi or cap attached to the wire array. The thickness of the bulk Bi cap on either side of the nanowire array is over  $300 \mu\text{m}$ . Two copper wires (gauge 36) were then attached to each Bi layer at each side of the nanowire array using silver epoxy<sup>29</sup> (see Fig. 2 inset). Low-temperature solder, such as Woods' metal, was avoided since it becomes superconductive at low temperatures ( $T_c \approx 8$  K) and shields the nanowire array from magnetic fields smaller than its critical field. Direct bonding of Bi to Cu electrodes at high temperatures leads to other shortcomings because Cu readily diffuses in Bi.<sup>14</sup> The contact resistances between the copper wires and the Bi layer is about  $0.1 \Omega$  over a contact area of  $0.15 \text{ mm}^2$ . The distance between contacts is between 0.3 and 0.5 mm. The resistance is calculated by  $R = (V^+ - V^-)/I$ , where  $(V^+ - V^-)$  is the voltage difference between the contacts and  $I$  is the current injected as shown in the inset of Fig. 2. This resistance is very small, around  $150 \mu\Omega$  at the

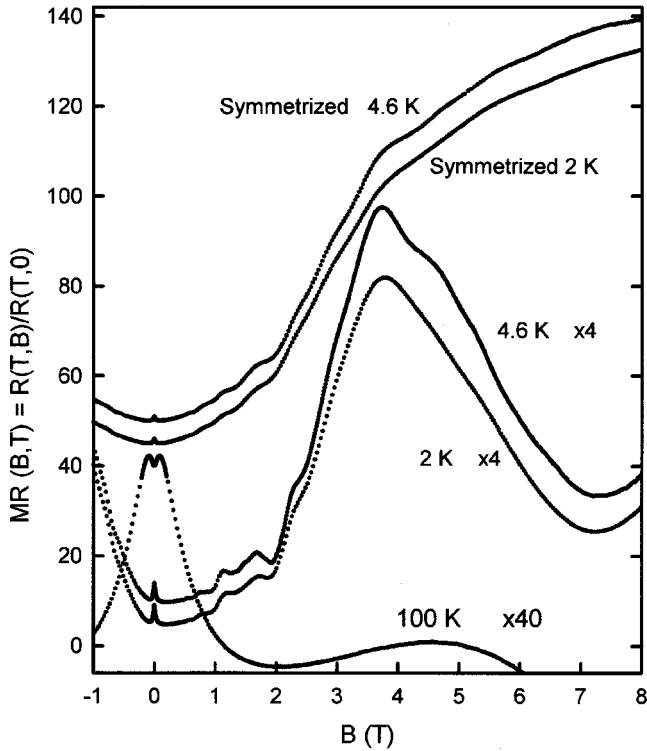


FIG. 3. Longitudinal magnetoresistance of the 200-nm (nominal) Bi wire array as a function of magnetic field at various temperatures. For clarity, the 2- and 4.6-K “as measured” curves have been displaced by 5 and 10. The 2- and 4.6-K symmetrized data have been displaced by 45 and 50.

lowest temperatures in this study and for a  $B$  value of 0 compared to the contact resistance between the copper wires and the Bi layer. This arrangement of electrodes has the drawback that the current injected by the current electrodes can be inhomogeneous across the nanowire array. This effect is similar to the phenomenon of current jetting in homogeneous samples.<sup>30</sup> The inhomogeneity is magnetic-field dependent since the layer material, which is polycrystalline Bi, has no longitudinal magnetoresistance and substantial transverse magnetoresistance and Hall effect. These effects and the details of the measurement of the magnetoresistance of the layer material (polycrystalline Bi) are discussed in the Appendix.

Figure 3 shows the longitudinal magnetoresistance (LMR) at various temperatures between 1.8 and 100 K for fields between  $-1$  and 8 T. The field is swept continuously through 0 via a bipolar current supply. The LMR contains an anti-symmetric contribution likely resulting from a Hall component due to current in the Bi caps that is not parallel to the field, and it also has a symmetric contribution that represents the actual magnetoresistance. The LMR observed is highly asymmetric [ $\text{MR}(B) < \text{MR}(-B)$  for  $B > 0$ ]. Figure 3 displays the “as measured” LMR for 2 and 4.6 K and the symmetric contribution  $\text{LMR}_{\text{sym}}$  for 2, 4.6, and 100 K. The symmetric LMR is obtained from the discrete sequence of experimental points by an interpolation algorithm [ $\text{LMR}_{\text{sym}}(B_i) = \text{LMR}(B_i) + \text{LMR}_{\text{int}}(-B_i)$ ] for all the experimental points, where the latter term is a linear interpolation

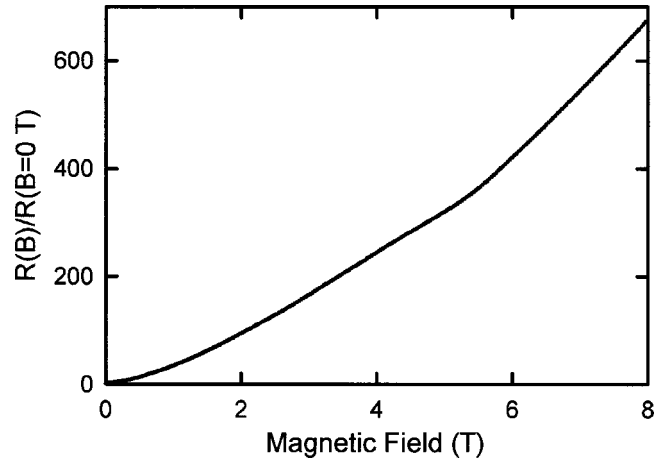


FIG. 4. Transverse magnetoresistance of the 200-nm (nominal) Bi wire array as a function of magnetic field at 4 K.

of the data points immediately below and above  $-B_i$ . The 100-K data display two broad maxima: a high-field maximum located at 5 T and a low-field maximum located at 0.12 T. The latter is believed to be a contact effect, as discussed in the Appendix. At low temperatures, 2 and 4.6 K, we found a broad maximum at  $B_c = 3.8$  T that is decorated with several peaks that, as discussed later, we ascribe to Aharonov-Bohm resonances for  $B < B_c$  and Shubnikov-de Haas resonances for  $B > B_c$ . A broad maximum in the LMR was also observed by Heremans *et al.*<sup>16</sup> in 200-nm-diameter wire arrays at 3 T and 70 K, the maximum temperature in that study; this maximum shifted to lower fields, 2 T at 20 K, and gradually disappeared at lower temperatures.

Figure 4 shows a typical curve for the nanowires’ transverse magnetoresistance with the field perpendicular to the wire axis (TMR) at  $T = 1.8$  K. The TMR is larger than the LMR at the same magnetic field. The transverse magnetoresistance  $R$  is a quadratic function of the magnetic field  $B$  at low magnetic fields:

$$\text{MR}(T) = \frac{R(T, B) - R(T, 0)}{R(T, 0)} = AB^2, \quad (2)$$

where the coefficient  $A$  is temperature dependent.  $A$  characterizes the carrier mobility, with a higher value indicating higher mobility.

At 2 K, we find that  $A = 50 \text{ T}^{-2}$  for  $B < 0.2$  T. At higher magnetic fields ( $0.2 < B < 3$  T), we find that  $\text{MR} = 580B^{1.4 \pm 0.1}$ . In Bi single crystals at low temperatures, the quadratic dependence applies only at very low fields ( $B < 10^{-4}$  T) and a  $B^{1.6}$  dependence is found for higher magnetic fields.<sup>31,32</sup> The extended range for the validity of Eq. (2) can be understood in terms of reduced mean free path. If the carrier mean free path at 4.2 K in single-crystal Bi is on the order of 0.4 mm and is on the order of the wire diameter (270 nm) for the nanowires of this study, the quadratic field dependence range of the wires’ TMR is expected to be larger by about 1500, which compares favorably with our observations. In comparison to our nanowires, the 200-nm-diameter sample in previous studies<sup>16</sup> had  $A = 0.1 \text{ T}^{-2}$ , indicating that

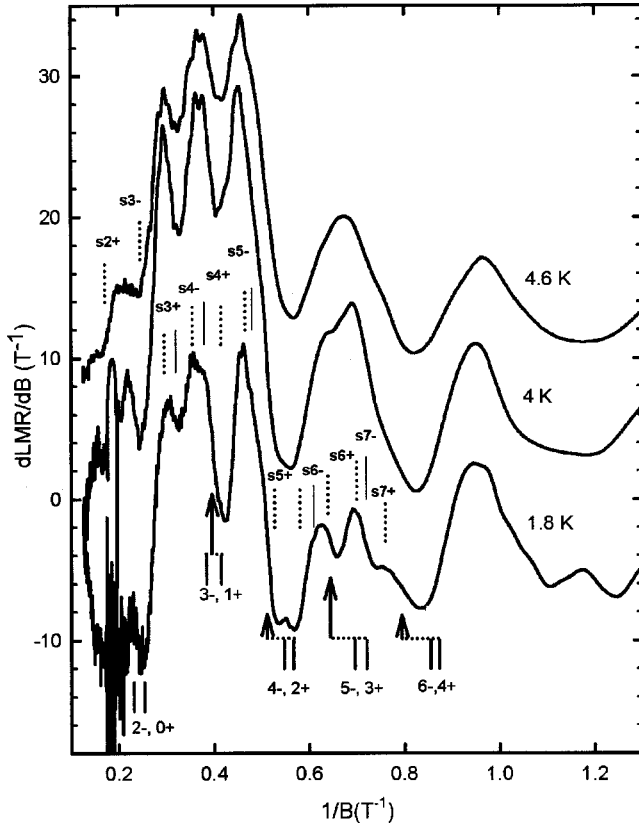


FIG. 5. Derivatives of the symmetrized longitudinal magnetoresistance of the 200-nm (nominal) Bi nanowire array at  $T=2$  and 4.6 K as a function of  $1/B$ . The lines and arrows indicate the various peaks discussed in the text.

our samples have much higher mobility. The polycrystalline Bi caps can potentially cause the quadratic coefficient of the TMR of the sample to be very large. This artifact was evaluated but comparison of the magnetic-field-dependent TMR of the nanowires (Fig. 4) with the TMR of a polycrystalline Bi sample (these measurements are discussed in the Appendix) shows that the TMR of the nanowires lacks the pronounced SdH oscillatory structure shown by the cap material. A single feature, or “bump,” at about 4 T is observed in the transverse magnetoresistance curve. This bump was also observed in Ref. 16 and is presumably connected to the broad local maximum observed in the LMR at the same magnetic field.

The bump in the symmetric LMR at around 4 T can be understood in terms of Chambers’ effect.<sup>4</sup> The carrier cyclotron radius is given by  $r_c = h k_F / 2\pi e B$ , where  $h$  is Planck’s constant,  $k_F$  is the carrier Fermi wave vector, and  $e$  is the electron charge. At low fields such that  $r_c > d/2$ , carrier scattering at the wire walls dominates and the resistance is high. As the field increases and the cyclotron radius is less than half the diameter ( $r_c < d/2$ ), scattering by the walls becomes ineffective and the resistance decreases. The magnetoresistance is therefore negative, and the effect is more pronounced for high-mobility carriers. However, if the bulk nanowire material has a small, but not zero, positive LMR, the resulting LMR shows a mixed behavior with a maximum occurring, very roughly, for a magnetic field  $B_c$  such that the

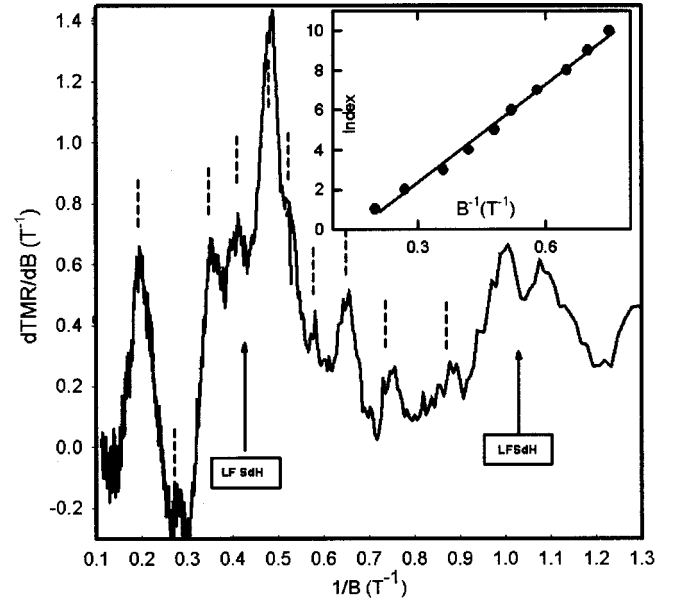


FIG. 6. Derivative of the transverse magnetoresistance of the 200-nm (nominal) Bi nanowire array at  $T=2$  K as a function of  $1/B$ . The lines and arrows indicate the various peaks discussed in the text. The inset shows hole peak positions.

cyclotron radius equals half the diameter ( $r_c = d/2$ ). Any misalignment would also result in a positive contribution to the magnetoresistance since the nanowires have a very large TMR.

The cyclotron masses for the trigonal orientation, found experimentally from studies of single-crystal bulk Bi,<sup>33–35</sup> are around  $m_{ce} = 0.065 m_0$  for electrons and  $m_{ch} = 0.067 m_0$  for holes with  $m_0$  being the free-electron mass. We can estimate the “cyclotron” Fermi wave vector in Chambers’ expression as  $k_{c,F} = 2\pi(2m_{ce}\gamma_F)^{1/2}/h$ , where  $\gamma_F = E_F(1 + E_F/E_G)$  with  $E_F$  being the Fermi energy,  $E_G$  being the gap energy, and with an average cyclotron mass of 0.066. Since  $E_F = 26$  meV and  $E_G = 15$  meV, we find that  $\gamma_F = 71$  meV and  $k_{c,F} = 3.2 \times 10^8/\text{m}$ . Thus, for an average wire diameter (e.g.,  $d = 270$  nm), we estimate that Chambers’ peak for electrons should appear at  $B = 1.6$  T, a value which is about 2.5 times lower than our experimental observation. For comparison, in Ref. 16, the theoretical estimate of  $B_c$  for  $d = 200$  nm is between three and ten times lower than their experimental value. Also, we find that the LMR maximum at 3.8 T in our samples becomes broader and shifts to higher magnetic fields with increasing temperatures, which may explain why the peak observed in Ref. 16 appears at a magnetic field higher than the theoretical estimate since, in that case, it was observed only at high temperatures.

We now discuss our observation of magnetoquantum oscillations. Shubnikov–de Haas (SdH) oscillations are due to the quantization of closed orbits (Landau levels). As the magnetic field is increased, the energy of the Landau level increases, and when its minimum value becomes equal to the Fermi energy, it is suddenly depopulated. The relaxation time for electron scattering is temporarily increased at this field value, giving rise to a dip in the magnetoresistance. The SdH

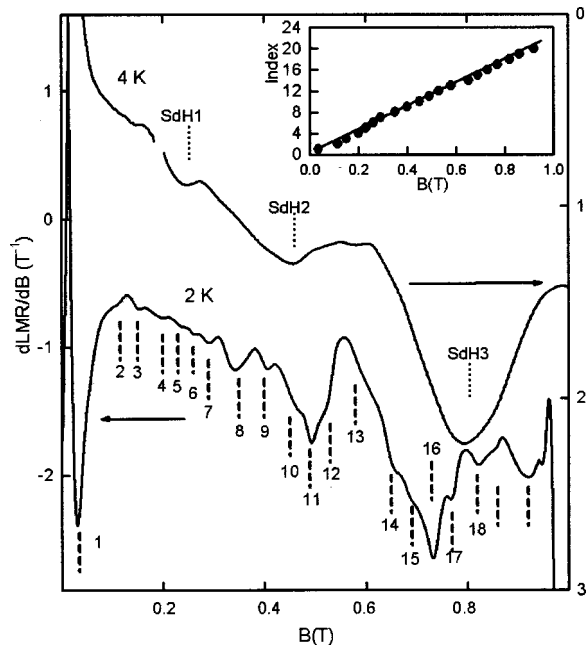


FIG. 7. Symmetrized longitudinal magnetoresistance of the 200-nm (nominal) Bi wire array at low magnetic fields and low temperatures. The peaks from AB oscillations are indicated with dashed lines. The inset shows the derivative minimum index as a function of magnetic field.

oscillations are periodic in  $1/B$ . Figures 5 and 6 show the derivative of the LMR and the TMR, respectively, versus  $1/B$  for our 270-nm Bi nanowires. Figure 5 presents the data for  $B > 1.3$  T at various temperatures and shows a number of minima and a number of short-period oscillations. The SdH minima in the LMR for hole carriers in a bulk Bi single crystal (which are split by spin-orbit interaction), with the magnetic field parallel to the trigonal axis, were observed by Smith *et al.*<sup>33</sup> and by Bhargava<sup>34</sup> via de Haas–van Alphen measurements. More recent cyclotron resonance measurements have been reviewed by Edelman.<sup>35</sup> The accepted value for the SdH period for hole carriers in bulk Bi is  $0.1575 \text{ T}^{-1}$ . The LMR of Bi nanowires at 1.8 K, shown in Fig. 5, shows evidence for holes. There is fair agreement between our peaks and the hole peaks in bulk Bi that are indicated in the figure. We note that our hole peaks become sharper for the lowest temperatures studied here, in the range  $0.25 < B < 0.5 \text{ T}^{-1}$ , indicating that the Dingle temperature ( $T_D$ ) is less than 2 K. Two of the prominent spin-split pairs of hole peaks are located at  $0.42$  and  $0.84 \text{ T}^{-1}$  (labeled in the figure as “3–, 1+” and “6–, 4+”) at high magnetic fields and low temperatures. The spacing of the hole peaks is  $0.135 \pm 0.01 \text{ T}^{-1}$ , smaller than the corresponding SdH spacing for holes in bulk Bi of  $0.157 \text{ T}^{-1}$ .

Having identified the hole peaks, it is then possible to identify a number of short-period ( $s$ ) oscillations between the hole peaks, which is suggestive of electrons. The electron oscillations are indicated with dashed lines. The measurement of SdH oscillations corresponding to electrons in bulk Bi for  $B \parallel$  trigonal axis has proven to be very elusive. Precise measurements of the SdH electron periods have been made

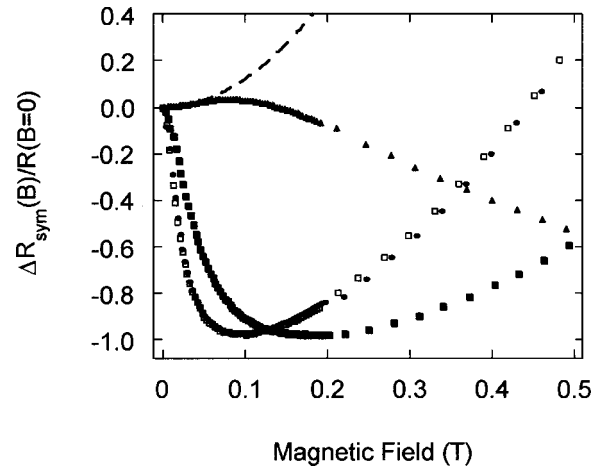


FIG. 8. Symmetric contribution to the longitudinal magnetoresistance around  $B=0$ . Full triangles correspond to a temperature of 100 K. The quadratic fit to the 100-K data,  $MR = MR_0 + A B^2$ , is shown with dashed lines. The symmetric contributions to the longitudinal magnetoresistance at 1.8, 4.6, and 20 K are represented with open squares, filled circles, and filled squares, respectively.

by using the de Haas–van Alphen method,<sup>34</sup> and cyclotron resonance measurements have been performed.<sup>35</sup> Edelman indicates that while the electron period for nanowires exactly along the trigonal direction is  $0.08 \text{ T}^{-1}$ , the period varies strongly with orientation: the effective mass changes by a factor of 2 for every  $10^\circ$  of separation from the trigonal direction. However, there are theoretically three branches of the electron-period curves that converge for  $H$  nearly parallel to the trigonal axis. Presumably, the resulting mixing and the presence of strong hole peaks made electrons very difficult to observe in SdH experiments in contrast to holes. Mixing between the electron and hole oscillations have also been reported.<sup>36</sup> In the experiments reported here, the short period can be followed over a wide range of inverse magnetic fields. The oscillation is indicated with full vertical lines in the cases where it is possible to make a clear identification. The period is found to be  $0.063 \pm 0.002 \text{ T}^{-1}$ . The Dingle temperature of the short period features appears to be higher than around 4 K because they overcome the hole features at 4 and 4.6 K. It is not possible to ascribe the short-period oscillations to electrons with certainty. Another possible origin for the short period is hole SdH from wires that are misoriented.

The intensity of the dips corresponding to the  $2^-$ ,  $0^+$  and  $4^-$ ,  $2^+$  labels in Fig. 5 is much larger than that of the  $3^-$ ,  $1^+$  levels. This trend continues at high temperatures and low magnetic fields where the hole SdH oscillation continues as a sequence of peaks with a period of approximately  $0.31 \pm 0.02 \text{ T}^{-1}$ . This sequence is more clearly observed for  $T = 4.6 \text{ K}$  and for  $B^{-1} > 0.6 \text{ T}^{-1}$ . One explanation for this undertone is that the density of states of Landau levels with odd  $n$  is larger than those of even  $n$ , but we know of no theoretical justification for such an effect. A more plausible origin for an SdH period of  $0.3 \text{ T}^{-1}$  may be that our nanowires have a distribution of angles relative to the Anapore surface normal and therefore with respect to the magnetic field. If the

degree of misalignment is as high as  $20^\circ$ , new electron SdH oscillations which have a reported period<sup>37</sup> of  $0.30 \text{ T}^{-1}$  should then be observable. This is consistent with the degree of misalignment of the nanowires as shown in Fig. 1; the misalignment is probably compounded by the difficulty in exactly aligning our small samples in the applied magnetic field. Assuming that we have a distribution of orientations, we can correct our estimate of the confinement-induced decrease of the SdH hole period. The angular variation of the hole periods in the binary plane has been measured,<sup>34</sup> and for a distribution of angles between  $20^\circ$  and  $-20^\circ$  around the trigonal direction, the average hole period is  $0.152 \text{ T}^{-1}$ . Therefore, since the observed holes' SdH period is  $0.135 \text{ T}^{-1}$ , we find a decrease in the hole SdH period  $\Delta P_{h,\parallel}$  of  $-0.017 \pm 0.01 \text{ T}^{-1}$  from the expected value for bulk Bi.

Figure 6 presents the derivative of the TMR data for  $B > 1.3 \text{ T}$  at  $1.8 \text{ K}$  and shows a number of short-period oscillations (*sp*) that are indicated with arrows. We also indicate the peaks that arise from a lower-frequency SdH oscillation. The SdH minima in the LMR for hole carriers in a bulk Bi single crystal, with the magnetic field perpendicular to the trigonal axis, were observed by Smith *et al.*<sup>33</sup> and by Bhargava.<sup>34</sup> The accepted value for the SdH spacing for hole carriers in bulk Bi is  $0.046 \text{ T}^{-1}$ . The data shown in Fig. 6 show evidence for holes with a period of  $0.055 \pm 0.004 \text{ T}^{-1}$ . The hole SdH period for  $B$  near the perpendicular to the trigonal axis is not a sensitive function of angle because spin splitting increases for orientations away from the binary-bisectrix plane. Therefore the observed hole period is larger than the expected value for bulk Bi ( $\Delta P_{h,\perp} = 0.009 \pm 0.004 \text{ T}^{-1}$ ). We find no evidence for possible electron SdH oscillations in the nanowires in the TMR data.

We do not believe that the observed oscillations result from a contribution from the Bi caps. A simple discrete circuit element model of our device, which includes resistive contributions from the longitudinal and transverse magnetoresistance of the Bi caps, has been used to estimate the contribution of the TMR of our Bi caps to the observed SdH oscillations in our LMR caps (see the Appendix). Assuming that the bulk LMR is negligible, it is found that the measured logarithmic field derivative of our device resistance  $R = (V^+ - V^-)/I$  has two contributions:

$$\frac{(dR/DB)}{R} = 2 \frac{(dR_{\text{NWA}}/dB)}{R_{\text{NWA}}} - \frac{(dR_a/dB)}{R_a}, \quad (3)$$

where  $R_{\text{NWA}}$  and  $R_a$  are the resistive contributions from the nanowires (with current parallel to the field) and from the Bi cap (with current perpendicular to the field), respectively. Our data for  $R_{\text{cap}}$  (see the Appendix) show that our observed SdH oscillations cannot be accounted for by a SdH contribution from the caps.

We note that our measured hole periods are inconsistent with the nanowire orientation along the direction (202) for the samples studied in Refs. 7, 8, 13, and 15. Therefore our

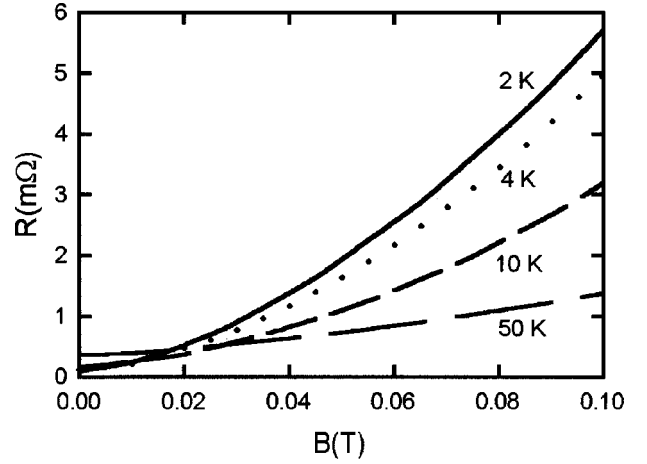


FIG. 9. Magnetic-field-dependent transverse ( $\mathbf{j} \perp \mathbf{B}$ ) resistance of the Bi contact layer material at various temperatures as indicated. The sample length is  $0.3 \text{ cm}$  and its cross section is  $10^{-3} \text{ cm}^2$ .

SdH data provide further confirmation for the  $C3$  trigonal orientation of our nanowires as determined through XRD measurements.<sup>14</sup>

In Fig. 7, we show the magnetic field derivative of the LMR versus magnetic field for temperatures of  $2$  and  $4 \text{ K}$ . We observe a number of inflections and peaks in the low-field ( $B \leq 1 \text{ T}$ ) LMR. The peak at  $B = 0$  can be understood in terms of a contact effect and will be discussed in the Appendix. As shown in the inset of Fig. 7, the positions of the minima in the range  $0.2\text{--}1 \text{ T}$  and at  $2 \text{ K}$  suggest oscillations which are periodic in  $B$ , with a periodicity ( $\Delta B_{\text{AB}}$ ) of  $0.045 \pm 0.003 \text{ T}$ . The oscillations were strongly damped at  $4 \text{ K}$  and were not observed at  $100 \text{ K}$ . The  $2\text{-K}$  results are consistent with Brandt's observation of AB whispering-gallery oscillations in the LMR of Bi nanowires with a magnetic-field periodicity corresponding to a field flux  $\Phi \approx \Phi_0$ . The authors' identification of the oscillations was based on a Fourier transform deconvolution of the data over an extensive range of magnetic fields ( $0 < B < 1.5 \text{ T}$  for  $d = 210 \text{ nm}$ ), as the oscillations are strongly damped for such small wire diameters. Additional work with wires that were  $560$  and  $800 \text{ nm}$  in diameter showed that the AB oscillations appear as a well-defined train of peaks over an extended range of magnetic field, and a study was made as a function of the angle between the nanowire and the magnetic field.<sup>8</sup> The intensity of the peaks was observed to increase for decreasing magnetic fields. For a wire cross section  $\pi d^2/4$ , where for each of our wires, the diameter was between  $235$  and  $310 \text{ nm}$ , such oscillations ought to appear with a period ranging from  $0.043$  to  $0.075 \text{ T}$ , which is to be compared to our experimental result of  $\Delta B_{\text{AB}} = 0.045 \pm 0.003 \text{ T}$ . Thus we infer that our observed oscillations originate in the large-diameter portion of the funnel and that the contribution from the small-diameter portion of the funnels is weak. This effect is consistent with the observation by Brandt that there is an increase in the damping of AB oscillations as the Bi nanowire diameter is decreased. This would explain both the observation of AB oscillations over an extended range and the low value of  $\Delta B_{\text{AB}}$ . The regular periodicity, sustained over

20 periods, suggests that these are not aperiodic Dingle oscillations.<sup>3</sup> In contrast to the study of AB oscillation in 560- and 800-nm single nanowires, the intensity of our AB oscillations is irregular (although we note that, on the average, the amplitude decreases with increasing magnetic field). This discrepancy is probably related to the large negative magnetoresistance which we observed and is related to contact effects, as discussed in the Appendix. Moreover, as the 4-K data in Fig. 7 show, SdH oscillations modulate the AB amplitude.

#### IV. DISCUSSION

The hole SdH periods are found to be modified from the accepted value for bulk Bi. The data in Figs. 5 and 6 on the hole Fermi surface can be interpreted in terms of the ellipsoidal model. The hole number density for an ellipsoidal Fermi surface is given by the equation<sup>34</sup>

$$p = (8/3\pi^{1/2})\Phi_0^{-3/2}(P_{h,\parallel}P_{h,\perp}^2)^{-1/2}. \quad (4)$$

For bulk Bi,  $P_{h,\parallel} = 0.157 \text{ T}^{-1}$  ( $B \parallel C3$ ) and  $P_{h,\perp} = 0.045 \text{ T}^{-1}$  ( $B \perp C3$ ), and one finds  $p = 3.0 \times 10^{17}/\text{cm}^3$ , while for 270-nm Bi nanowires, we find that  $p = 2.6 \pm 0.3 \times 10^{17}/\text{cm}^3$ , an overall decrease in the spatial hole density ( $p$ ) of 13%. The substantial decrease of the spatial hole density indicates that the effect of confinement is to make the wire approach the semiconducting state. Also, our observations indicate that the ellipsoidal shape is modified by confinement to render it more spherical. The SdH period of the hole doublets ( $P_H$ ) are given by  $2\mu_B/[m_{\text{ch}}(E_o - E_F)]$ , where  $m_{\text{ch}}$  is anisotropic. From Eq. (3), we find that  $p \sim (E_o - E_F)^{3/2}$  and that the observed decrease of the spatial charge density of holes can be attributed to a decrease of the gap energy with respect to the Fermi energy of 1.05 meV. Overall, neglecting the observed anisotropy modifications, the hole periods are 5% larger than those in bulk Bi.

Confinement causes the energies associated with the transverse motion to be quantized, and the lowest energy level is increased, roughly, by  $\Delta E$  [Eq. (1)]. Evaluation of this expression for the parameters for the trigonal direction and for  $d = 270 \text{ nm}$  gives  $\Delta E_o = 0.84 \text{ meV}$ , which is in very good agreement with our measurements. Here, we have assumed that the Fermi energy does not change upon confinement because a complete study of this issue is beyond the scope of this study.

Typically, the crystal structure of individual Bi nanowires is rhombohedral, with the same lattice parameters as that of bulk Bi, and the crystalline orientation varies somewhat depending upon growth conditions. In most cases reported to date, the nanowires are oriented in a direction close to the normal to the (202) lattice plane of the rhombohedral crystal structure of Bi.<sup>7,8,13,16</sup> In contrast, for our high-pressure injection fabrication conditions (pressure and temperature schedule), the wires in the array were predominantly oriented with the trigonal crystal axis along the wire length.<sup>14</sup> This orientation is close to being perpendicular to the crystalline orientation of the nanowires in Brandt's study. The trigonal crystalline orientation is well suited for investigation of the

LMR of the nanowire array, as it can be shown from symmetry considerations that the LMR for bulk Bi is null along the trigonal direction. This favorable orientation contributes in part to our ability to observe the very weak AB oscillations.

It should be noted that measurements on nanowire array samples made of 200-nm (nominal) Anopore without Bi caps also yield SdH oscillations and that these periods also indicate confinement effects similar to those presented here. However, due to the large contact resistance associated with the silver epoxy-nanowire interface which is several ohms, the data is of lower quality than presented here.

At low temperatures, we observed a number of whispering-gallery AB oscillations of the LMR at low fields ( $H < 1 \text{ T}$ ) with a periodicity ( $\Delta B_{\text{AB}}$ ) of 0.045 T. These oscillations are interpreted to originate from electron orbits inscribing magnetic flux loops of  $\Delta\Phi = \Phi_0$ , where  $\Phi_0 = hc/e$ . The mean free path is estimated to be longer than  $1 \mu\text{m}$ . This path length is still much shorter than the 1000- $\mu\text{m}$  mean free path of free carriers in bulk Bi at low temperatures, possibly because grazing orbits involve close contact between carriers and the wire wall. A theoretical study of the AB effect by Bogachek and Gogadze<sup>38</sup> has shown that it is a low-temperature effect and that the resonances are stable for temperatures ( $T$ ) less than  $T_{\text{BG}} \approx h^2 k_F / (2\pi^3 m d)$ , where  $m$  is the carriers' effective mass. For our parameters, we estimate that  $T_{\text{BG}} \approx 4 \text{ K}$  for electrons in these Bi nanowires, which is in agreement with our observation that the AB oscillations are strongly damped at 4 K and disappear completely for  $T = 100 \text{ K}$ . We hope that measurements presented here will stimulate further theoretical developments.

#### V. SUMMARY

We have presented a study of the electrical transport properties of 270-nm-diameter bismuth nanowire arrays embedded in an alumina matrix which are capped with layers of bulk Bi that have low contact resistance. The results of our measurements present evidence for semiclassical and quantum size effects. Shubnikov-de Haas resonances from the quantization of the energy of carriers into Landau levels present evidence for confinement effects, namely shifts on the position of the holes' Landau levels, and subtle size effects, namely complex orbits involving scattering with the nanowire walls and orbits in the bulk of the wire. At low magnetic fields, the longitudinal magnetoresistance (LMR) displays pronounced oscillations whose periods and amplitudes are in fair agreement with theoretical predictions for the AB effect in whispering-gallery modes of electrons with the long mean free path. The observation of these phenomena in nanowire arrays, where the measured oscillations represent the average response of over  $10^9$  individual nanowires only 270 nm in diameter, suggests that single nanowires will exhibit even more pronounced quantum effects.

### ACKNOWLEDGMENTS

We thank Dr. Nikolaeva and Prof. Gitsu of the Institute of Solid State of the Academy of Sciences of Moldavia for valuable advice. The authors also thank Dr. M. Erwin of the U.S. Army Research Laboratory at Adelphi, MD., for the SEM measurements. The work was supported by the Division of Materials Research of the U.S. National Science Foundation under Grant No. NSF-0072847, the NSF grant program ‘‘Research in Undergraduate Institutions’’ (NSF-0097733), and by the Division of Materials of the U.S. Army Research Office under Grant No. DAAD4006-MS-SAH and instrumentation Grant No. DAADI9-00-1-0033.

### APPENDIX: FOUR-POINT PROBE METHOD AND CURRENT JETTING

The peaks at  $B=0$  T at low temperatures and at  $B=0.12$  T at 100 K, shown in Figs. 3 and 8, show the symmetric contribution to the longitudinal magnetoresistance at low fields and various temperatures. These peaks are believed to result from the anisotropy of the magnetoresistance of the bulk Bi contact material. The phenomenon is called current jetting in bulk materials and causes anomalous longitudinal magnetoresistance as measured with four aligned point contacts when the current contact is nonuniformly distributed on the sample cross section.<sup>30</sup> The nanowire array magnetoresistance is obtained from the calculation  $(V^+ - V^-)/I$ , where  $V^+$  and  $V^-$  are the potentials at the voltage contacts and  $I$  is the current injected in the current contacts as indicated in the inset of Fig. 2. If the resistance of the Bi layer is negligible,  $(V^+ - V^-)/I = R_{\text{NWA}}$ , where  $R_{\text{NWA}}$  is the resistance of the nanowire array and includes the contact resistance of the nanowires to the bulk Bi layer. However, even though the resistivity of the bulk Bi layer material at  $B=0$  is very small at low temperatures, in the presence of a magnetic field, the resistivity in the direction perpendicular to the magnetic field ( $\rho_{\perp}$ ) increases by many orders of magnitude (the resistivity in the direction of the magnetic field  $\rho_{\parallel}$  remains negligible). The effective lateral resistance between the voltage and current contacts increases rapidly with an applied magnetic field. Consequently, the current flows unevenly across the nanowire array: as the magnetic field is increased, the current in the nanowires will become larger in the section of the nanowire array directly between the current contacts and smaller in the section between the voltage contacts. In order to correctly model this effect, we have studied the magnetoresistance of a sample of bulk Bi from the area adjacent to the nanowire array in the injection reactor. This material has experienced similar time-dependent temperatures and pressures, and thus its crystalline structure should be the same as that of the Bi contact layers at either side of the nanowire array sample. The temperature-dependent resistivity of this material is presented in Fig. 2. We find that our results for the resistivity are consistent with those obtained for similar materials in the literature.<sup>39</sup> For example, the residual resistivity of our Bi contact layer material is  $1.86 \mu\Omega$  cm, while the reported residual resistivities of polycrystalline Bi range between 2 and  $100 \mu\Omega$  cm. We measure a

room-temperature resistivity of  $1200 \mu\Omega$  cm, which compares favorably with other reported values. We also measured the Hall effect and the field-dependent longitudinal and transverse resistivities  $\rho_{\parallel}$  and  $\rho_{\perp}$  with the magnetic field both parallel and perpendicular to the direction of current flow, by using Putley’s five-contact arrangement.<sup>39</sup> The value for  $\rho_{\parallel}(B)/\rho(B=0)$  of the Bi contact material was measured at low temperatures and was found to be close to 1. Figure 9 shows the resistance  $R_{\perp}(B)$  of a rod of the polycrystalline Bi contact layer material of length  $L=3$  mm and  $0.001 \text{ cm}^2$  in cross section for  $B<0.1$  T at various temperatures. The transverse magnetoresistance,  $\text{MR}_{\perp} = \rho_{\perp}(B)/\rho(B=0)$ , is large; i.e., for a magnetic field of 0.1 T,  $\text{MR}_{\perp}(1.8 \text{ K})=60$  and exhibits a  $B^{1.6}$  magnetic-field dependence in the range of interest ( $B<0.2$  T). A fit to the expression  $\text{MR}_{\perp} = 1 + CB^{1.6}$  shows that the coefficient  $C$  increases for decreasing temperatures. Although still large, the transverse magnetoresistance of polycrystalline Bi is smaller than that of Bi single crystals due to a reduction of the electronic mean free path.

For a longitudinal magnetic field ( $B$  parallel to the length of the nanowires), we can disregard the resistance of the Bi contact layer material in the direction of the magnetic field and consider only the large changes of the lateral resistance of this Bi layer. Each set of contacts on each side of the sample (as shown in the inset in Fig. 2) occupies roughly one-half the area of the nanowire array. This assumption is consistent with the size of our contacts and the size of our sample. The resistance of the silver epoxy contacts themselves is neglected on account of their thickness and (measured) negligible magnetoresistance. The effective resistance between the current and voltage contacts at each side of the array,  $R_a$ , is determined by the resistance of the 0.3-mm-long layer of polycrystalline Bi material that bridges the gap between the current and voltage contacts.  $R_a$  is in series with the resistance of the nanowire array; it is a function of temperature and increases manyfold with application of the longitudinal magnetic field since it is effectively oriented perpendicular to the magnetic field. For  $R_a \ll R_{\text{NWA}}$ , the measured resistance is  $(V^+ - V^-)/I = R_{\text{NWA}}$ . However, if  $R_a > R_{\text{NWA}}$ , the measured resistance is  $(V^+ - V^-)/I = 2(R_{\text{NWA}})^2/R_a < R_{\text{NWA}}$ ,<sup>40,41</sup> because the current in the nanowires is larger in the section of the nanowire array directly between the current contacts and smaller in the section between the voltage contacts. Since  $R_a = R_{a,0} + R_{a,0}CB^{1.6}$ , we find that  $(V^+ - V^-)/I = 2(R_{\text{NWA}})^2[R_{a,0} + R_{a,0}CB^{1.6}]^{-1}$ , which explains the LMR peak which appears at  $B=0$  and also at the sharpening of the peak at low temperatures since the coefficient ( $C$ ) of the contact layer magnetoresistance increases for decreasing temperatures.

Because of the contact effects, SdH oscillations in the magnetoresistance of the bulk polycrystalline material are potentially relevant to the discussion of SdH oscillations of the nanowire array that were discussed in the study. Our measurements on the bulk polycrystalline material show that its transverse magnetoresistance presents oscillations in the range  $0.1\text{--}1.3 \text{ T}^{-1}$ , that is, in the range presented in Fig. 5. However, since these oscillations have a periodicity of  $0.137 \pm 0.01 \text{ T}^{-1}$  and their breadth is equal to the period, the SdH oscillations of the bulk polycrystalline material do not cause the peaks displayed in Fig. 5.

- <sup>1</sup>N. Garcia, Y. H. Kao, and M. Strogan, Phys. Rev. B **5**, 2029 (1972).
- <sup>2</sup>D. H. Reneker, Phys. Rev. Lett. **1**, 440 (1958).
- <sup>3</sup>R. B. Dingle, Proc. R. Soc. London, Ser. A **201**, 545 (1950); S. S. Nedorezov, Zh. Eksp. Teor. Fiz. **56**, 299 (1969) [Sov. Phys. JETP **29**, 164 (1969)].
- <sup>4</sup>R. G. Chambers, Proc. R. Soc. London, Ser. A **202**, 378 (1950).
- <sup>5</sup>R. B. Dingle, Proc. R. Soc. London, Ser. A **212**, 47 (1956).
- <sup>6</sup>A. G. Scherbakov, E. N. Bogachev, and U. Landman, Phys. Rev. B **53**, 4054 (1996).
- <sup>7</sup>N. B. Brandt, D. V. Gitsu, A. A. Nikolaeva, and Y. G. Ponomarev, Zh. Eksp. Teor. Fiz. **72**, 2332 (1977) [Sov. Phys. JETP **45**, 1226 (1977)]; N. B. Brandt, D. B. Gitsu, V. A. Dolma, and Ya. G. Ponomarev, *ibid.* **92**, 913 (1987) [*ibid.* **65**, 515 (1987)].
- <sup>8</sup>N. B. Brandt, E. N. Bogachev, D. V. Gitsu, G. A. Gogadze, I. O. Kulik, A. A. Nikolaeva, and Ya. G. Ponomarev, Fiz. Nizk. Temp. **8**, 718 (1982) [Sov. J. Low Temp. Phys. **8**, 358 (1982)].
- <sup>9</sup>N. W. Ashcroft and N. D. Mermin, in *Solid State Physics* (Harcourt Brace College Publishers, Fort Worth, 1976), Chap. 14.
- <sup>10</sup>M. Lu, R. J. Zieve, A. van Hulst, H. M. Jaeger, T. F. Rosenbaum, and S. Radelaar, Phys. Rev. B **53**, 1609 (1996).
- <sup>11</sup>M. Gurvich, J. Low Temp. Phys. **38**, 777 (1980).
- <sup>12</sup>T. E. Huber and M. J. Graf, Phys. Rev. B **60**, 16 880 (1999).
- <sup>13</sup>Y. Lin, X. Sun, and M. S. Dresselhaus, Phys. Rev. B **62**, 4610 (2000); Z. Zhang, X. Sun, M. S. Dresselhaus, J. Y. Ying, and J. Heremans, *ibid.* **61**, 4850 (2000).
- <sup>14</sup>T. E. Huber, M. J. Graf, and C. A. Foss, Jr., J. Mater. Res. **15**, 1816 (2000).
- <sup>15</sup>T. E. Huber, M. J. Graf, C. A. Foss, Jr., and P. Constant, in *Thermoelectric Materials 2000—The Next Generation for Small-Scale Refrigeration and Power Generation Applications*, edited by T. M. Tritt, G. S. Nolas, G. Mahan, M. G. Kanatzidis, and D. Mandrus, Mater. Res. Soc. Symp. Proc. No. 626 (Materials Research Society, Pittsburgh, 2001).
- <sup>16</sup>J. Heremans, C. M. Thrush, Y. Lin, S. Cronin, Z. Zhang, M. S. Dresselhaus, and J. F. Manfield, Phys. Rev. B **61**, 2921 (2000).
- <sup>17</sup>K. Liu, C. L. Chien, and P. C. Searson, Phys. Rev. B **58**, R14 681 (1998).
- <sup>18</sup>H. M. Swartjes, A. P. van Gelder, A. G. M. Jansen, and P. Wyder, Phys. Rev. B **39**, 3086 (1989).
- <sup>19</sup>C. A. Hoffman, J. R. Meyer, F. J. Bartoli, A. Di Venere, X. J. Yi, C. L. Hou, H. C. Wang, J. B. Ketterson, and G. K. Wong, Phys. Rev. B **48**, 11 431 (1993).
- <sup>20</sup>H. J. Goldsmid, in *Electronic Refrigeration*, 2nd edition (Pion, London, 1986), pp. 104–110.
- <sup>21</sup>L. D. Hicks and M. S. Dresselhaus, Phys. Rev. B **47**, 12 727 (1993).
- <sup>22</sup>C. A. Huber and T. E. Huber, J. Appl. Phys. **64**, 6588 (1988).
- <sup>23</sup>Whatam Laboratory Division, Clifton, NJ.
- <sup>24</sup>T. E. Huber, O. Anakoya, and M. Ervin, J. Appl. Phys. **92**, 1337 (2002).
- <sup>25</sup>T. E. Huber, P. Constant, K. Celestine, M. Bouffard, and M. J. Graf, in *Proceedings of the 20th International Conference on Thermoelectrics*, edited by J. Zhang (IEEE, Piscataway, 2001), p. 356.
- <sup>26</sup>Y. V. Sharvin, Zh. Eksp. Teor. Fiz. **48**, 984 (1965) [Sov. Phys. JETP **21**, 655 (1965)].
- <sup>27</sup>E. N. Bogachev, A. G. Scherbakov, and U. Landman in *Nanowires*, Vol. 340 of *NATO Advanced Study Institute, Series E: Applied Sciences*, edited by P. A. A. Serena and N. Garcia (Kluwer, Dordrecht, 1997), p. 35.
- <sup>28</sup>J. Tersoff, Appl. Phys. Lett. **74**, 2122 (1999).
- <sup>29</sup>Silver Epoxy E4110-PFC from Epoxy Technology, Billerica, MA.
- <sup>30</sup>A. B. Pippard in *Magnetoresistance in Metals* (Cambridge University Press, Cambridge, England, 1989), Chap. 2.
- <sup>31</sup>R. N. Zitter, Phys. Rev. **127**, 1471 (1962).
- <sup>32</sup>S. Mase, S. Von Molnar, and A. W. Lawson, Phys. Rev. **127**, 1030 (1962).
- <sup>33</sup>G. E. Smith, G. A. Baraf, and J. M. Rowell, Phys. Rev. **135**, A1118 (1964).
- <sup>34</sup>R. N. Bhargava, Phys. Rev. **156**, 785 (1967).
- <sup>35</sup>V. S. Edelman, Zh. Eksp. Teor. Fiz. **68**, 257 (1975) [Sov. Phys. JETP **41**, 125 (1975)].
- <sup>36</sup>L. S. Lerner, Phys. Rev. **127**, 1480 (1962).
- <sup>37</sup>R. J. Balcombe and A. M. Forrest, Phys. Rev. **151**, 550 (1966).
- <sup>38</sup>B. N. Bogachev and G. A. Gozadze, Zh. Eksp. Teor. Fiz. **63**, 1839 (1972) [Sov. Phys. JETP **36**, 973 (1973)].
- <sup>39</sup>C. Uher and W. P. Pratt, Jr., Phys. Rev. Lett. **39**, 491 (1977).
- <sup>40</sup>E. H. Putley, in *The Hall Effect and Semiconductor Physics* (Dover, New York, 1960).
- <sup>41</sup>The measured resistance  $(V^+ - V^-)/I$  can be calculated via a simple model that includes two resistances in parallel, each one representing the resistance of the half of the nanowire array that is near the current or voltage contacts and of value  $2R_{\text{NWA}}$ , which are connected in a closed loop via two other resistances, each one representing the Bi contact layer resistance  $R_a$ . The current flows into the loop at the junction between the resistance  $(2R_{\text{NWA}})$  near the current contact and  $R_a$ , and exits out of the loop at the junction between the same resistance  $(2R_{\text{NWA}})$  and the other  $R_a$ . The voltage  $(V^+ - V^-)$  is measured across the other resistance  $(2R_{\text{NWA}})$ . Thus  $(V^+ - V^-)/I = 2(R_{\text{NWA}})^2/(2R_{\text{NWA}} + R_a)$ .